



وحرارة نوعية بالإضافة إلى قياس هبوط الضغط، درجات حرارة سطح الأنابيب والمائع داخل الأنابيب، معدل التدفق ومقدار الفيض الحراري.

وفي حالة الموائع متناهية الدقة فإن نسبة عدد نسلت كانت (7.5) باستخدام (CuO) والشريط الملتوي (clockwise-counter clockwise) بنسبة التواء (TR = 4) وعدد رينولد (2490) وتركيز (φ = 3%) ، أما أعلى معامل الأداء الحراري فكان (3.9) لنفس الظروف. لوحظ إن مقدار التحسين في انتقال الحرارة يعتمد بشكل كبير على تركيز الجزيئات المتناهية في الصغر و نوعها.

تم الحصول على معادلات ارتباط لعدد نسلت و معامل الاحتكاك بدلالة عدد رينولد ونسبة الالتواء والتركيز لكل أنواع الموائع متناهية الدقة المستخدمة.

## INTRODUCTION

For more than 100 years, scientists and engineers have made great efforts to enhance the inherently poor thermal conductivity of liquids by adding solid particles in liquids. (Maxwell, 1873) presented a theoretical basis for predicting the effective conductivity of suspensions [1].

The term **Nanofluids** coined by **Choi** [2] are engineering colloids made of a base fluid and nanoparticles that are between 1 to 100 nm in diameter consists of metal or metal oxide nanoparticles , such as copper and alumina, and the base fluid is usually a conductive fluid, such as water , ethylene glycol and others [1, 3].

**Masuda et al.** [1] were the first to conduct experiment to show that there was alteration in the values of thermal conductivity and viscosity of liquids containing dispersed ultra fine particles of 13 nm size. Subsequent researches [2, 4, 5] showed that the nanofluids exhibited higher thermal conductivity even for low concentration of suspended nanoparticles.

**Sharma et al.** [6] conducted experiments to evaluate heat transfer coefficient and friction factor characteristics of Al<sub>2</sub>O<sub>3</sub>/water nanofluid flowing in a tube with twisted tape inserts under transition range of flow. Their results also showed a considerable enhancement of convective heat transfer with Al<sub>2</sub>O<sub>3</sub> nanofluids compared to water. Using the same experimental setup, **Sundar and Sharma** [7] evaluated the heat transfer coefficient and friction factor characteristics of Al<sub>2</sub>O<sub>3</sub>/water nanofluid flowing in a tube with twisted tape inserts under turbulent flow.

**Sajadi**, [8] experimentally investigated turbulent heat transfer behavior of titanium dioxide/water nanofluid in a circular pipe with volume fraction range (0.05-0.25%) and Reynolds number range (5000-30000). The results indicated that addition of small amounts of nanoparticles to the base fluid augmented heat transfer remarkably and the pressure drop of nanofluid was slightly higher than that of the base fluid.

**Khalid Faisl Sultan** [9] conducted a study to investigate the theoretical and experimental heat transfer and flow of nanofluids through a horizontal and an inclined circular tube heated by an axial uniform heat flux under thermally and hydro dynamically fully developed region with laminar flow. Using Al (25nm), Al<sub>2</sub>O<sub>3</sub> (30nm) and CuO (50nm) in distilled water nanofluids. The range of Reynolds number was chosen to be (100 – 900), range of Rayleigh number was between (1×10<sup>3</sup> – 4×10<sup>6</sup>) and concentrations were from (0.25 – 2.5 vol %). The results showed that the values of Nusselt number ratio were evaluated to be (45%, 31%, 25%) for the three nanofluids (Al, Al<sub>2</sub>O<sub>3</sub>, CuO) – distilled water, respectively.

**Syam Sundar, et al.**, [10] experimentally evaluated the convective heat transfer coefficient and friction factor characteristics of Fe<sub>3</sub>O<sub>4</sub> magnetic nanofluid for flow in a circular tube is evaluated experimentally in the range of 3000 < Re < 22,000 and the volume concentration range of 0 < φ < 0.6% using a stable colloidal suspension of magnetite (Fe<sub>3</sub>O<sub>4</sub>) nanoparticles of average

diameter 36 nm. Nanofluid heat transfer is higher compared to water and increases with volume concentration.

**Heyhat, et al., [11]** experimentally studied the heat transfer coefficient and friction factor of the  $Al_2O_3$  in distilled water nanofluids flowing in a horizontal tube under laminar flow conditions. The experiments have been done under the constant wall temperature condition with volume concentrations of 0.1–2 vol. %. The results show that the heat transfer coefficient of nanofluid is higher than that of the base fluid and increased with increasing the Reynolds number and particle concentrations.

**Jianli Wanga, et al. [12]**, investigated experimentally the heat transfer and pressure drop of nanofluids containing carbon nanotubes in a horizontal circular tube with Reynolds number range (30–200). A considerable enhancement in the average convective heat transfer is observed compared with the distilled water. For the nanofluids with volumetric concentration of 0.05% and 0.24%, the heat transfer enhancement is 70% and 190% at Reynolds number of about 120 respectively.

**Naik, et al., [13]** Heat transfer and friction factor characteristics of water/propylene glycol based CuO nanofluids flowing in a plain tube were investigated experimentally under constant heat flux boundary condition. Experiments were conducted with 0.025, 0.1 and 0.5% volume concentration and Reynolds numbers range (1000–10000). The effect of twisted tape with twist ratios range of (0 to 15) and nanofluids was studied. The experimental results show a significant increment in the heat transfer coefficient of CuO nanofluids. The heat transfer coefficient increased up to 27.95% in the 0.5% CuO nanofluid in plain tube and with TR= 5 it is further increased to 76.06% over the base fluid.

### **The Experimental Test Rig**

The experimental loop was designed for convective heat transfer in turbulent flow domain. The horizontal test section was a copper tube of (1.9cm) (3/4 in) diameter and a (1.5 m) length which is electrically heated by a coil made from tungsten material of (10 m) long and (4 mm) width with (1000 W) heating power connected to an AC power supply to generate heat flux, the tube has a hydrodynamic fully developed length of (1 m). Insulation of rock wool type with (1.9cm) (3/4 in) internal diameter and (6.35cm) (2.5 in) outer diameter used to insulate the (1.5 m) test section. The electrical circuit of heating element consists of variac (2000W) to adjust the heater input power as required, while a digital Wattmeter (type Dm – 9020) was used to measure the power consumed by the heater. Thirty two thermocouples (T–type) were used to measure the temperatures along the outer surface of the tube at the heated test section with a space distance of (5 cm) between each one. Two thermocouples were immersed in the flow to measure the inlet and outlet temperatures of the fluid in the test section. All thermocouples were connected to data acquisition system used to record the thermocouples readings and display to personal computer directly.

Two flow meters were used to measure flow rate; the first one of range (0.8–7 l/min) and the other of range (4–38 l/min). The flow meter was connected in parallel and positioned just after the circulating pump.

U-tube manometer and the inclined manometer were used to measure the pressure drop across the (1.5 m) length test section. The U-tube manometer graduation is (75 cm) and connected to the pressure tap at the inlet and outlet of the test section, while the inclined manometer of range (0 - 250 Pa) was used to measure the low pressure drop in the testing section. Figure (1) shows the Schematic diagram of experimental test rig.

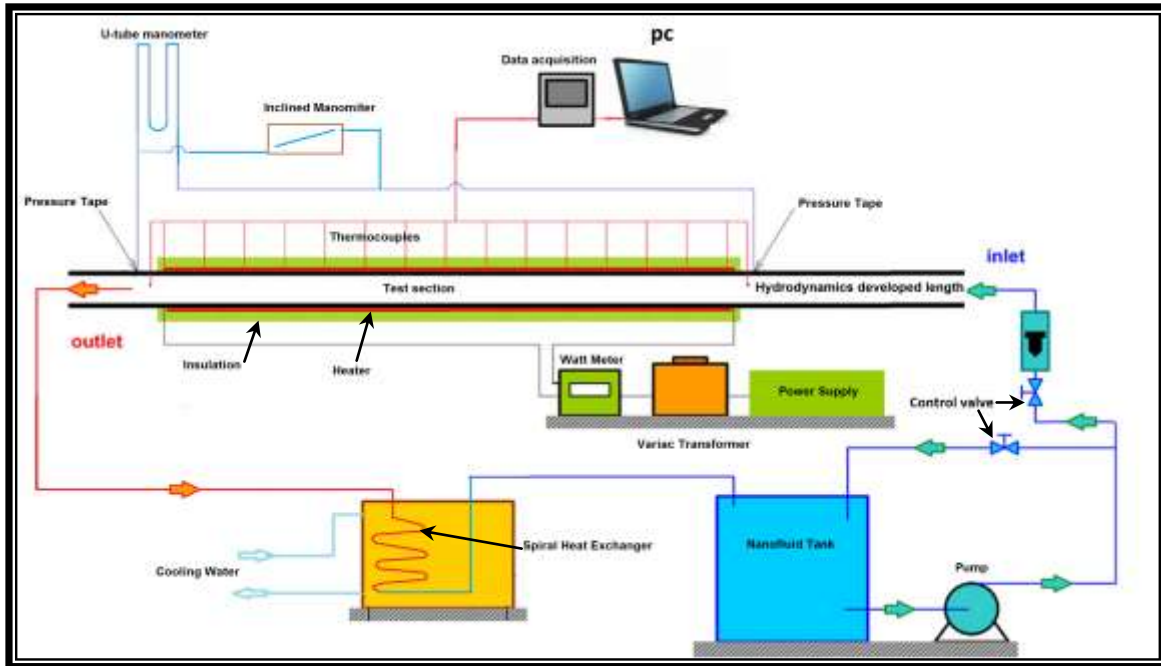


Figure (1) Schematic diagram of Experimental apparatus

### Twisted Tape

The twisted tapes were manufactured from a metal strip of finite length twisted with different pitches and twist ratios (the pitch is the distance required for the strip to rotate  $180^\circ$ ), and the twist ratio (TR) is the ratio of pitch to the width of the tape. The twisted tape was fabricated from an Aluminum strip of length (150cm), width (17 mm) and thickness (0.70 mm).

Three configurations of the twisted tape were fabricated which are:

- 1) Typical twisted tape figure (2).
- 2) Twisted tape with V- cut: The dimensions of the V-cut are taken from Murugesan, [14] who found the optimum cut depth ratio and width ratio as (DR=0.43, WR=0.34), respectively for all twist ratios, as shown in figure (3) where:

$$DR = \frac{e_d}{W} \tag{1}$$

$$WR = \frac{e_w}{W} \tag{2}$$

The V-cut is located in each pitch in opposite direction to the previous one.

- 3) Clockwise - counter clockwise: The clockwise-counter clockwise twisted tape changes its direction of rotation every two pitch distance (i.e., the tape rotate  $360^\circ$  in the clockwise direction along the distance "2P", and then it rotates in the counter clockwise direction  $360^\circ$  for the next distance "2P", this sequence will continue until the test section length reached, as shown in figure (4).

Each twist tape was fabricated with three twist ratios (TR = 4, 6, 8), as shown in Figures (2) (3) and (4).

$$TR = \frac{P}{W} \quad (3)$$

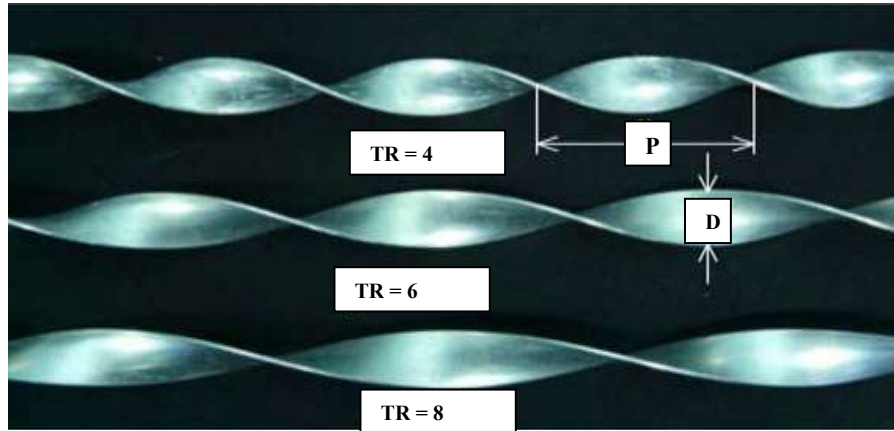


Figure (2) Twisted tape

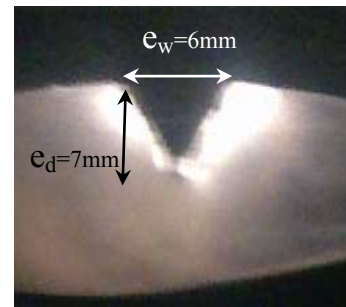


Figure (3) Twisted tape with V- cut



Figure (4) Clockwise - counter clockwise twisted tape

### Preparations of Nanofluids

In order to get a stable and durable suspension, with low agglomeration of particles, a two – step method was selected to prepare the nanofluids [15, 16, and 17].

Nanofluid samples were prepared for different concentrations by dispersing pre – weighed quantities of dry particles in distilled water. The mixtures were then subjected to ultrasonic mixing [60 kHz, 500W, High sonic, England] for (2 hours) to break up any particle aggregates. The concentrations used in the experiments are ( $\phi = 0, 0.01, 0.05, 0.1, 0.5, 1, 2, 3\%$  by volume).

The nanoparticles used in the preparation of nanofluids are:

1. Zirconium Oxide { $ZrO_2$  (80 nm)} provided from (Nanoshel Intelligent Materials provider Ltd. USA).
2. Aluminum Oxide Nanoparticle ( $\gamma Al_2O_3$ , gamma, 99+%, 20 nm).

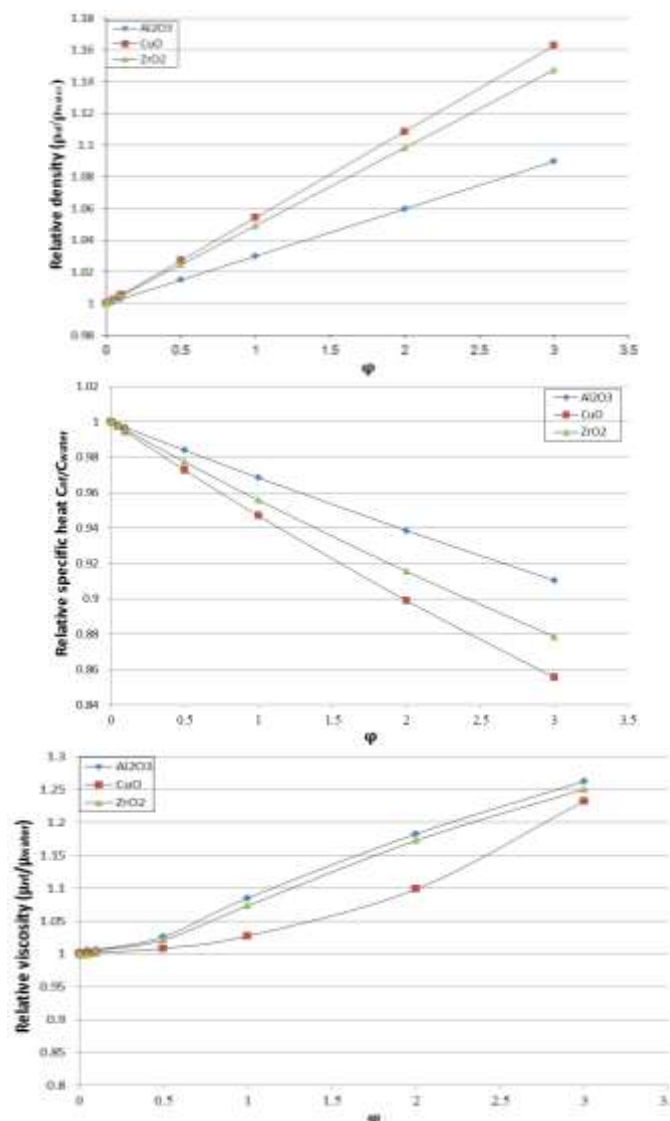
- Copper Oxide Nanoparticle (CuO, 99%, 40nm) both provided from (US Research Nanomaterials, Inc. USA).

### Measured Properties of nanofluid

The measured properties of the water – based  $ZrO_2$ ,  $Al_2O_3$ , CuO nanofluids are the dynamic viscosity ( $\mu$ ) is measured using Brook Field Digital Viscometer (Model Dv-E).

The specific heat is obtained using (ESD– 201) type apparatus.

The density was by weighing a sample volume of (500 ml) with different concentrations for each type of nanofluid, and dividing the values of weight by volume. Figure (5) gives the results of measurements.



Figures (5) shows measured properties of the water – based  $ZrO_2$ ,  $Al_2O_3$ , CuO Nanofluids at 25°C compared with that of pure water.

Duo to the difficulty of measuring the thermal conductivity, it was calculated using empirical formula by Vajjha [18], which is formulated for the three types of nanofluids.

$$k_{nf} = \frac{k_p + 2k_{bf} - 2(k_{bf} - k_p)\varphi}{k_p + 2k_{bf} + (k_{bf} - k_p)\varphi} k_{bf} + 5 \times 10^4 \beta \varphi \rho_{bf} C_{bf} \sqrt{\frac{KT}{\rho_p d_p}} f(\varphi) \tag{4}$$

$$f(\varphi) = (2.821 \times 10^{-2} \varphi + 3.917) + (-3.0669 \times 10^{-2} \varphi - 3.91123 \times 10^{-3}) \tag{5}$$

**Experimental Calculations**

**A) Heat Transfer coefficient of the Nanofluid**

The heat flux on the tube outer surface is given by:

$$Q_{heater} = \text{Power of heater} \tag{6}$$

The amount of the heat transferred from the heating wire to the nanofluid is given by:

$$Q_{fluid} = \dot{m}_{nf} \times C_{nf} \times (T_o - T_{in}) \tag{7}$$

T<sub>o</sub>, T<sub>in</sub> inlet and outlet temperature of the nanofluid at the test section, respectively in figure (6).

The heat balance between the nanofluid (Q<sub>fluid</sub>) and heat input (Q<sub>heater</sub>) was found to be within 3.0% for all runs. That is:

$$\left| \frac{Q_{heater} - Q_{fluid}}{Q_{heater}} \right| < 3\% \tag{8}$$

The heat flux in figure (6) is given by

$$q = \frac{Q_{fluid}}{A_s} = \frac{Q_{fluid}}{\pi DZ} \tag{9}$$

Where: (A<sub>s</sub>) is the surface area of the tube, (D) is the diameter of the pipe and (Z) is the length of the pipe.

The local heat transfer coefficient is calculated as follows using the heat flow shown in figure (6):

1. Starting from the known values {  $\dot{q}$ , T<sub>so</sub>(z) }
2. Using the conduction equation in the cylinder to calculate {T<sub>si</sub>(z)} [19]:

$$\dot{q} = \frac{Q_{fluid}}{A_s} = \frac{2\pi k \Delta Z [T_{so}(z) - T_{si}(z)]}{\pi D \Delta Z \times \ln\left(\frac{r_o}{r_i}\right)} = \frac{2k [T_{so}(z) - T_{si}(z)]}{D \times \ln\left(\frac{r_o}{r_i}\right)} \tag{10}$$

3. Also, from the energy balance in the tube, the mean temperature of nanofluid can be expressed by:

$$T_o(z + \Delta z) = T_{in}(z) + \frac{\dot{q} \times \pi DZ}{\dot{m}_{nf} \times C_{nf}} \tag{11}$$

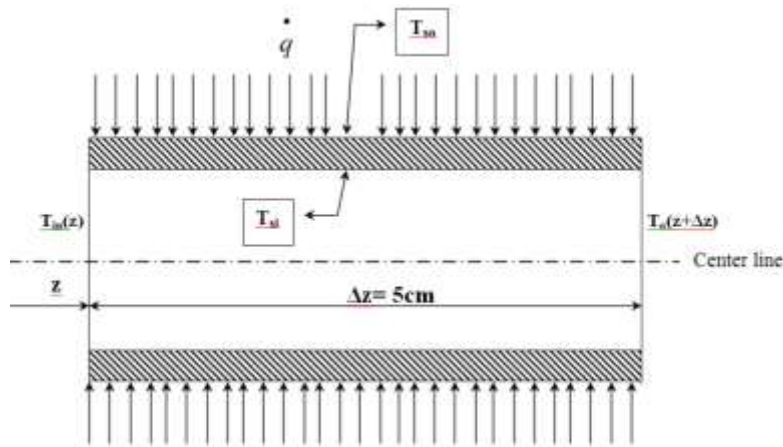


Figure (6) Section of the pipe of length  $\Delta z$  and at distance  $(z)$

Thus, the local heat transfer coefficient becomes:

$$h(z) = \frac{q}{T_{sf}(z) - T(z)} \quad (12)$$

Where:  $T(z) = (T_{in}(z) + T_o(z + \Delta z)) / 2$  is the nanofluid bulk temperature.

The local Nusselt Number has been calculated from the following equation:

$$Nu(z) = \frac{h(z)D}{k_{nf}} \quad (13)$$

The average value of Nusselt number in the thermal fully developed region can be expressed by:

$$\overline{Nu} = \frac{1}{L} \int_0^L Nu(z) dz \quad (14)$$

And, the Reynolds number is

$$Re = \frac{\rho_{nf} w D}{\mu_{nf}} \quad (15)$$

### B) Pressure drop calculation

Based on the practically measured pressure drop, Darcy friction factor can be calculated using the expression [20]:

$$f = \frac{\left(\frac{\Delta p}{L}\right) D}{\rho w^2 / 2} \quad (16)$$

### Validation of Experimental Test Rig

In order to verify the test facility and the data obtained, heat transfer and pressure drop of a plain tube of (1.5 m) long as a test section were investigated. Figure (7) shows the Nusselt number verses Reynolds number for fully developed turbulent flow inside a plain tube using distilled water as the working fluid for the present test and the well know empirical correlation of Dittus –Boelter equation [19] equation (17).

$$Nu = 0.023 Re^{0.8} Pr^{0.3} \quad (17)$$

The present heat transfer results of test facility are in good agreement with the above equation with maximum deviation of (7.6 %). Figure (7) shows the agreement of friction factor with published data of Blasius equation [20], equation (18), with maximum deviation of (9.7%).

$$f = 0.316Re^{-0.25} \tag{18}$$

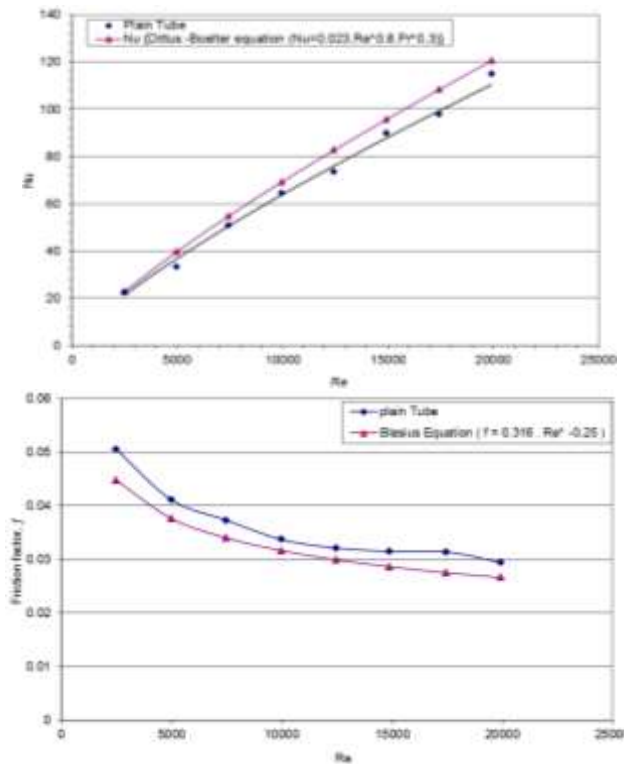


Figure (7) the effect of Reynolds number on Nusselt number with Dittus –Boelter equation and friction factor with Blasius equation for distilled water.

### Results and Discussion

The variation in Nusselt number with Reynolds number for the plain tube in comparison with the three types of twisted tape (typical twisted tape, twisted tape with V-cut, clockwise-counter clockwise) and with twist ratios (TR = 4, 6, 8) is shown in figure (8), respectively. In general, the Nusselt number increases as the Reynolds number increases for all the ranges of Reynolds number and types of twisted tape. Nusselt number increases when twist ratio decreases for all types of twisted tape used, as shown in figure (8), and (TR=4) gives the highest Nusselt number. Also, the clockwise-counter clockwise twisted tape gives the highest Nusselt number among the twisted tape types, for all twist ratios (TR=4, 6, 8).

The experimental results clearly show that nanoparticles suspended in water enhance the heat transfer. The local values of Nusselt number along the tube were used in the calculation of the overall Nusselt number of the tube as stated above. Figure (9) shows the variation of the average Nusselt number with Reynolds number in a plain tube for the three types of nanofluids at different concentrations. It is noted that the enhancement of heat transfer greatly depend on nanoparticle

type, CuO nanofluid shows the highest Nusselt number. As the concentration increases the Nusselt number increases because the effective thermal conductivity of nanofluid increases with increasing volume fraction of the nanoparticles, which is explained by Brownian motion of the nanoparticles, molecular – level layering of the liquid at liquid/particle interface (wettability). Enhanced thermal conductivity reduces resistance to thermal diffusion in the laminar sub layer of the boundary layer.

The Nusselt number for the typical twisted tape is higher than plain tube, for twisted tape with V-cut is higher than typical twisted tape and clockwise-counter clockwise twisted tape is higher than V-cut twisted tape for all types of nanofluids as shown in figure (10). Also, the Nusselt number for Al<sub>2</sub>O<sub>3</sub> is higher than ZrO<sub>2</sub> and for CuO is higher than Al<sub>2</sub>O<sub>3</sub> for all types of twisted tape and nanofluid concentration.

The enhancement in the heat transfer (the Nusselt number ratio)  $(Nu_{nanofluid}/Nu_{plain tube})$  is shown in figure (11) for plain tube. The maximum enhancement in the heat transfer for CuO was (3.7) at Reynolds number (2490) and concentration ( $\phi=3\%$ ), for Al<sub>2</sub>O<sub>3</sub> was (2.5) and for ZrO<sub>2</sub> was (2.4), both at Reynolds number (4981) and concentration ( $\phi=3\%$ ).

For tube with twisted tapes, figures (12), the maximum enhancement in the heat transfer for CuO was (7.5), for Al<sub>2</sub>O<sub>3</sub> was (6.5) and for ZrO<sub>2</sub> was (6.3), all of them occurred with clockwise-counter clockwise twisted tape and twist ratio (TR = 4) at Reynolds number (2490) and concentration ( $\phi=3\%$ ).

The enhancement in heat transfer coefficient in nanofluid is attributed to the effective thermal conductivity of nanofluid solution. The heat transfer coefficient is given as  $(k/\delta t)$ , where ( $\delta t$ ) is the thickness of thermal boundary layer. This means that the enhancement of thermal conductivity of nanofluid and/or decreasing thermal boundary layer thickness increases the heat transfer coefficient. Also, it seems that the thermal boundary layer thickness of nanofluid is smaller than that of the base fluid. In addition, the thermal dispersion due to the inherent random motion of particles contributes to this enhancement. As a result, the temperature gradient at the wall becomes steeper, and the heat transfer rate at the wall increases.

Heat transfer enhancement index or thermal performance factor is one of the key parameters necessary to define the heat transfer augmentation performance. The equation proposed by Eiamsa-ard et al. [21, 22] for constant pumping power is given by:

$$\eta = \frac{\left(\frac{Nu_{nanofluid}}{Nu_{plain tube}}\right)}{\left(\frac{f_{nanofluid}}{f_{plain tube}}\right)^{\frac{1}{3}}} \tag{19}$$

In general, the thermal performance factor above unity indicates that the effect of heat transfer enhancement is more dominant than the effect of rising friction and vice versa.

Figure (13) shows the variation in thermal performance factor with Reynolds number for the three types of nanofluids in plain tube. The maximum thermal performance factor for CuO was (2.7) with Reynolds number (2490) and ( $\phi =3\%$ ), and for Al<sub>2</sub>O<sub>3</sub> was (1.9) and ZrO<sub>2</sub> was (1.8) at Reynolds number (4981) and ( $\phi=3\%$ ).

For tube with twisted tapes, the maximum thermal performance factor for CuO was (3.7) and for Al<sub>2</sub>O<sub>3</sub> was (3.3) with clockwise-counter clockwise twisted tape, and for ZrO<sub>2</sub> was (3.4) with the typical twisted tape and twist ratio (TR = 4) at Reynolds number (2490) and ( $\phi =3\%$ ), figure (14).

The obtained data for Nusselt number and friction factor are related with Re, Pr,  $\phi$  and TR for the three types of nanofluids through the following correlations:

$$Nu = a_1 Re^{a_2} Pr^{a_3} (1 + \phi)^{a_4} TR^{a_5} \tag{20}$$

$$f = b_1 Re^{b_2} (1 + \phi)^{b_3} TR^{b_4} \tag{21}$$

For (Re=2490-20100), (Pr=5.5-6.5), ( $\phi$ =0.01-3%).

The values of constants and the deviations are given in Table (1) and (2).

**Table (1) Values of factors for eq. (20)**

**Plain tube**

Nanofluid	a <sub>1</sub>	a <sub>2</sub>	a <sub>3</sub>	a <sub>4</sub>	Deviation
CuO-distilled water	0.0159	0.6922	1.1906	0.5433	± 10%
Al <sub>2</sub> O <sub>3</sub> -distilled water	0.0365	0.78	0.2	0.57	± 10%
ZrO <sub>2</sub> - distilled water	0.017	0.701	1.1	0.4802	± 9.1%

**Typical twisted tape**

Nanofluid	a <sub>1</sub>	a <sub>2</sub>	a <sub>3</sub>	a <sub>4</sub>	a <sub>5</sub>	Deviation
CuO-distilled water	0.7303	0.586	0.079	0.453	-0.332	± 7%
Al <sub>2</sub> O <sub>3</sub> -distilled water	0.18	0.68	0.28	0.31	-0.378	± 8.2%
ZrO <sub>2</sub> - distilled water	0.399	0.648	0.109	0.423	-0.388	± 9%

**Twisted tape with V-cut**

Nanofluid	a <sub>1</sub>	a <sub>2</sub>	a <sub>3</sub>	a <sub>4</sub>	a <sub>5</sub>	Deviation
CuO-distilled water	0.938	0.580	0.128	0.455	-0.477	± 8.5%
Al <sub>2</sub> O <sub>3</sub> -distilled water	0.19	0.7	0.28	0.3	-0.283	± 9%
ZrO <sub>2</sub> - distilled water	0.508	0.639	0.197	0.418	-0.551	± 7%

**Clockwise-counter clockwise twisted tape**

Nanofluid	a <sub>1</sub>	a <sub>2</sub>	a <sub>3</sub>	a <sub>4</sub>	a <sub>5</sub>	Deviation
CuO-distilled water	2.611	0.486	0.357	0.329	-0.682	± 7.5%
Al <sub>2</sub> O <sub>3</sub> -distilled water	0.35	0.68	0.18	0.35	-0.37	± 10%
ZrO <sub>2</sub> - distilled water	1.156	0.568	0.4	0.3089	-0.742	± 9%

**Table (2) Values of factors for eq. (21)**

**Plain tube**

Nanofluid	b <sub>1</sub>	b <sub>2</sub>	b <sub>3</sub>	Deviation
CuO-distilled water	1.617	-0.407	0.412	± 7.5%
Al <sub>2</sub> O <sub>3</sub> -distilled water	0.4	-0.24	0.3	± 10%
ZrO <sub>2</sub> - distilled water	1.327	-0.3919	0.321	± 9.2%

**Typical twisted tape**

Nanofluid	b <sub>1</sub>	b <sub>2</sub>	b <sub>3</sub>	b <sub>4</sub>	Deviation
CuO-distilled water	12.34	-0.433	0.194	-0.598	± 7.3%
Al <sub>2</sub> O <sub>3</sub> -distilled water	14.436	-0.446	0.1762	-0.639	± 8.5%
ZrO <sub>2</sub> - distilled water	13.44	-0.433	0.14	-0.679	± 9.5%

**Twisted tape with V-cut**

Nanofluid	b <sub>1</sub>	b <sub>2</sub>	b <sub>3</sub>	b <sub>4</sub>	Deviation
CuO-distilled water	57.25	-0.547	0.347	-0.817	± 8%
Al <sub>2</sub> O <sub>3</sub> -distilled water	62.95	-0.554	0.316	-0.853	± 9%
ZrO <sub>2</sub> - distilled water	66.63	-0.557	0.267	-0.887	± 7%

Clockwise-counter clockwise twisted tape

Nanofluid	$b_1$	$b_2$	$b_3$	$b_4$	Deviation
CuO-distilled water	41.72	-0.5	0.25	-0.766	+ 7%
Al <sub>2</sub> O <sub>3</sub> -distilled water	47	-0.508	0.215	-0.812	+ 10%
ZrO <sub>2</sub> - distilled water	50.8	-0.509	0.169	-0.874	+ 9%

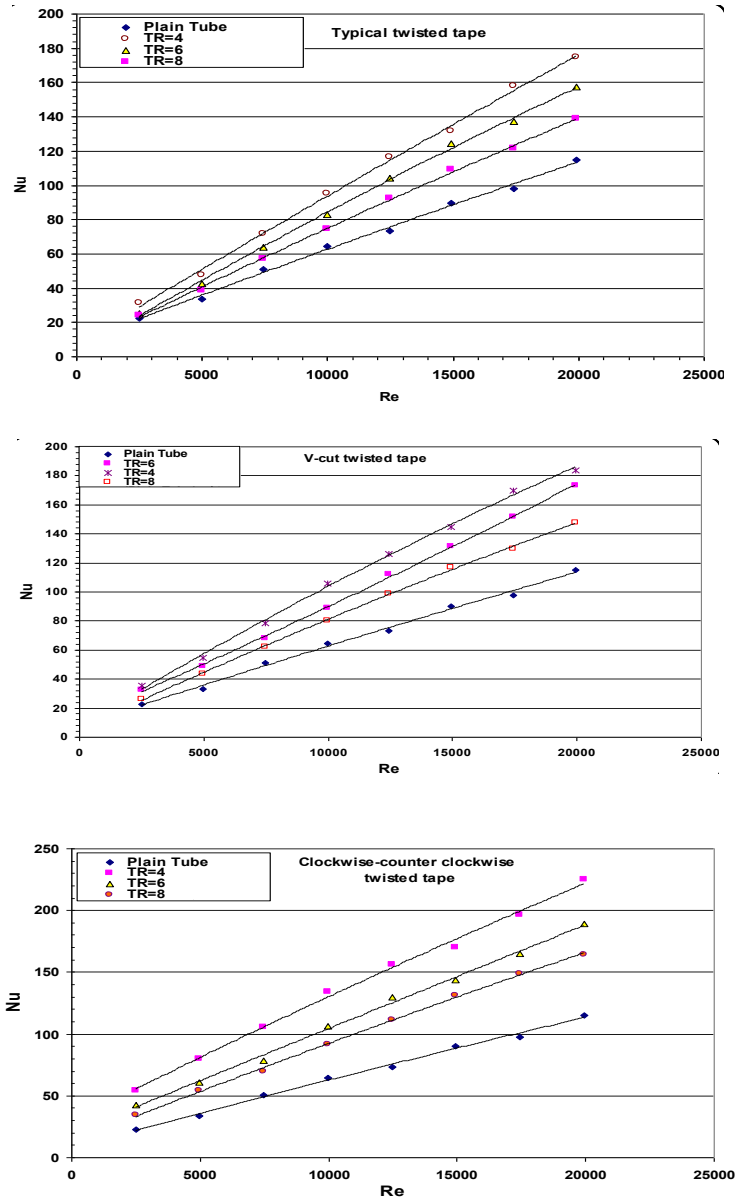


Figure (8) The effect of Reynolds number and twist ratio for three types of twisted tape on Nusselt number for distilled water.

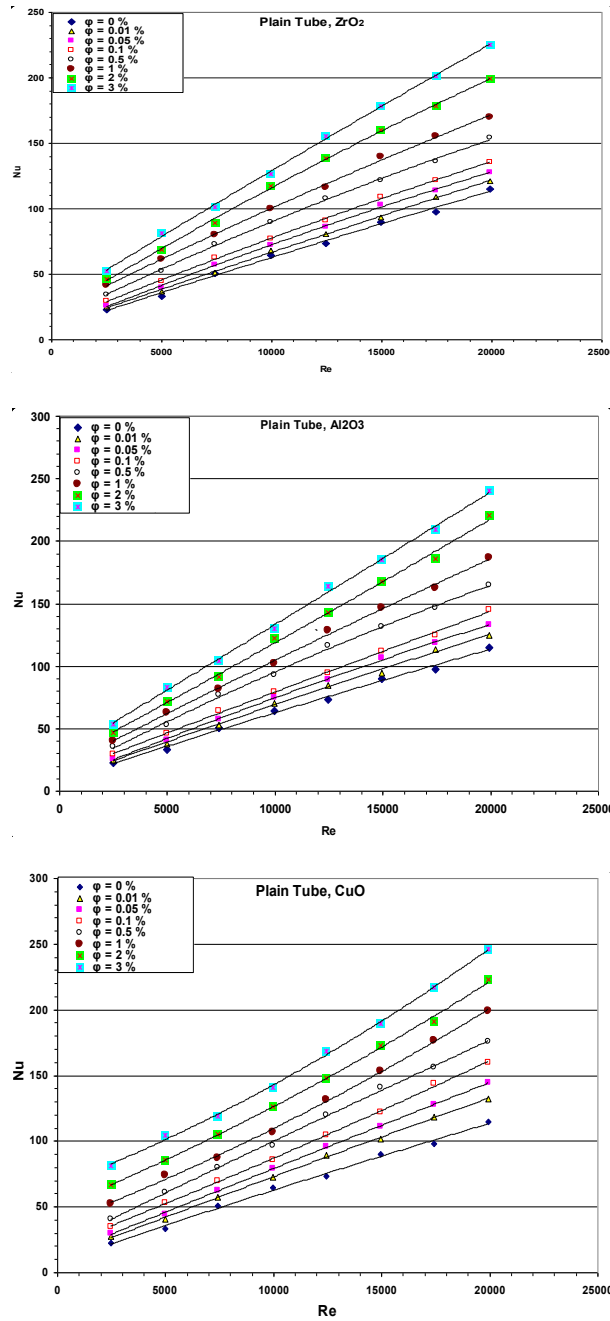


Figure (9) The effect of Reynolds number on Nusselt number for ZrO<sub>2</sub>, CuO, Al<sub>2</sub>O<sub>3</sub> nanofluid for different concentrations in a plain tube.

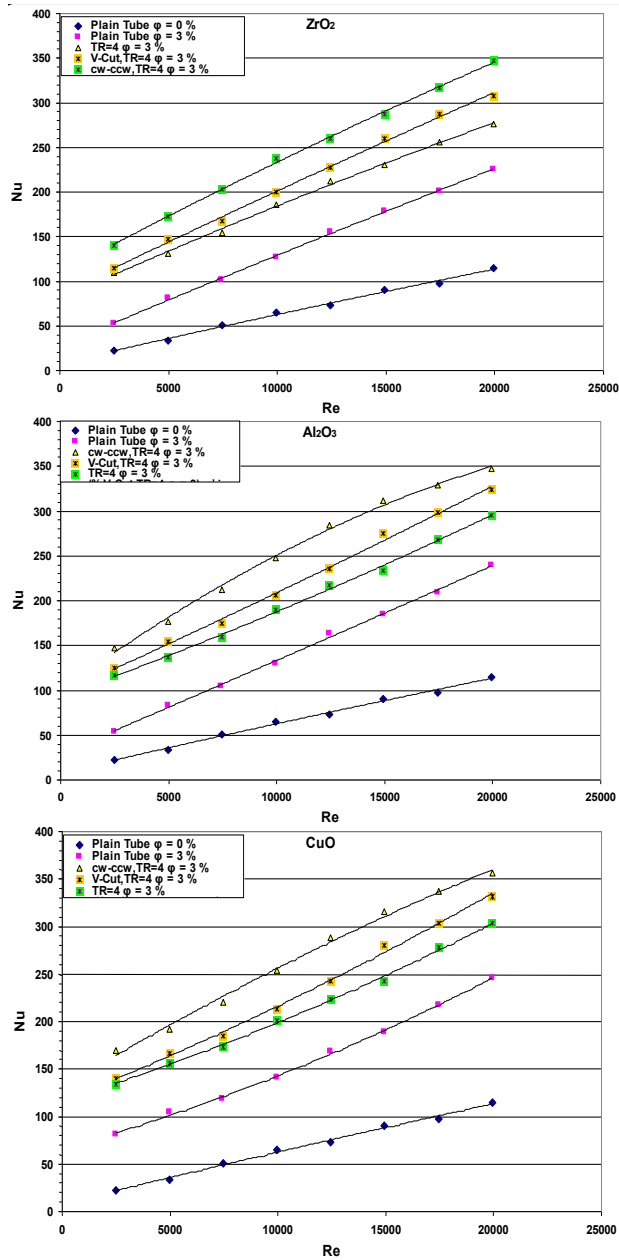


Figure.(10) The effect of Reynolds number on Nusselt number for three types of nanofluid and concentrations ( $\phi=3\%$ ) with different twisted tape types.

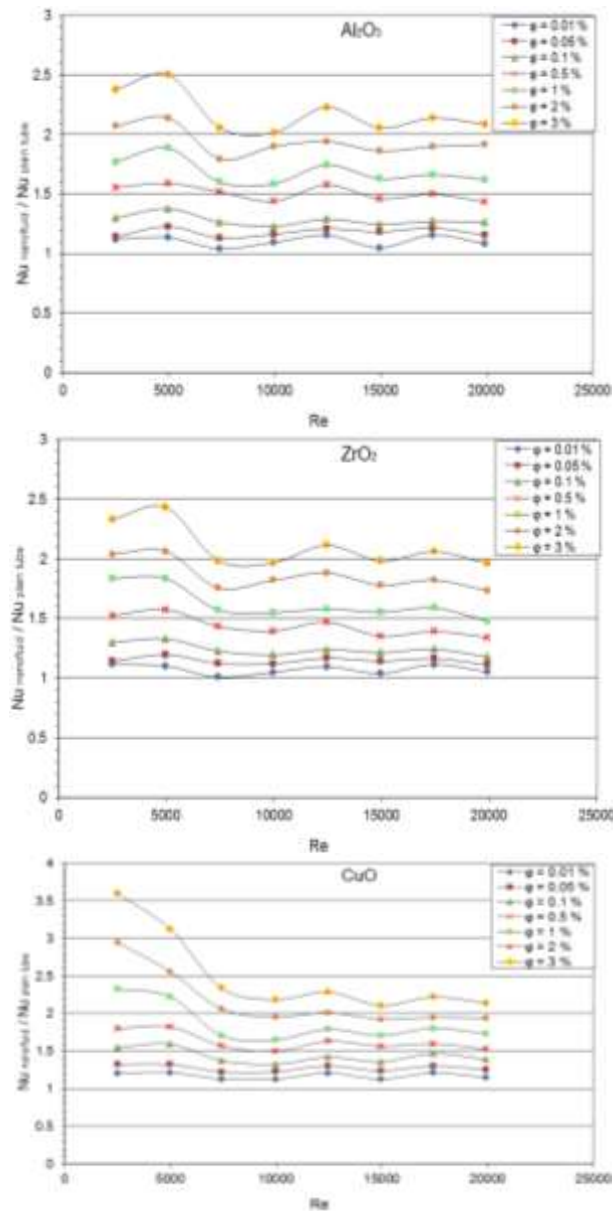


Figure (11) The effect of Reynolds number and twist tape type on Nusselt number ratio  $(Nu_{nano\ fluid} / Nu_{plain\ tube})$  for  $ZrO_2$ ,  $CuO$ ,  $Al_2O_3$  nanofluid and for different concentrations in a plain tube.

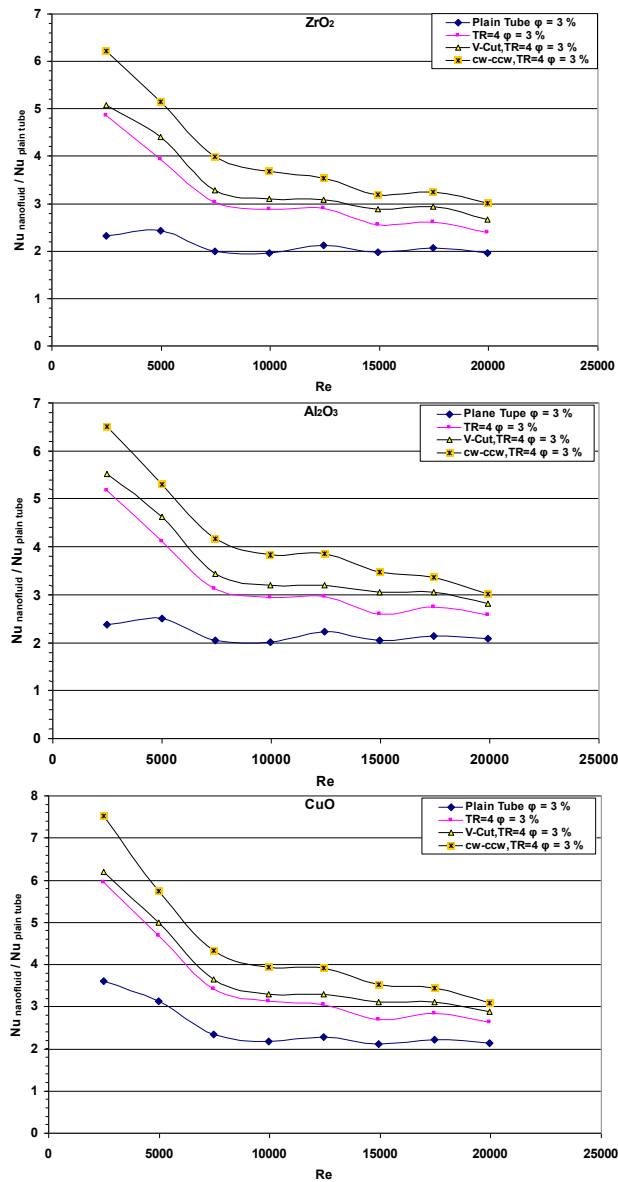


Figure.(12) The effect of Reynolds number and twist tape type on Nusselt number ratio  $(Nu_{nanofluid}/Nu_{plain tube})$  for three types of nanofluid and concentrations ( $\phi = 3\%$ )

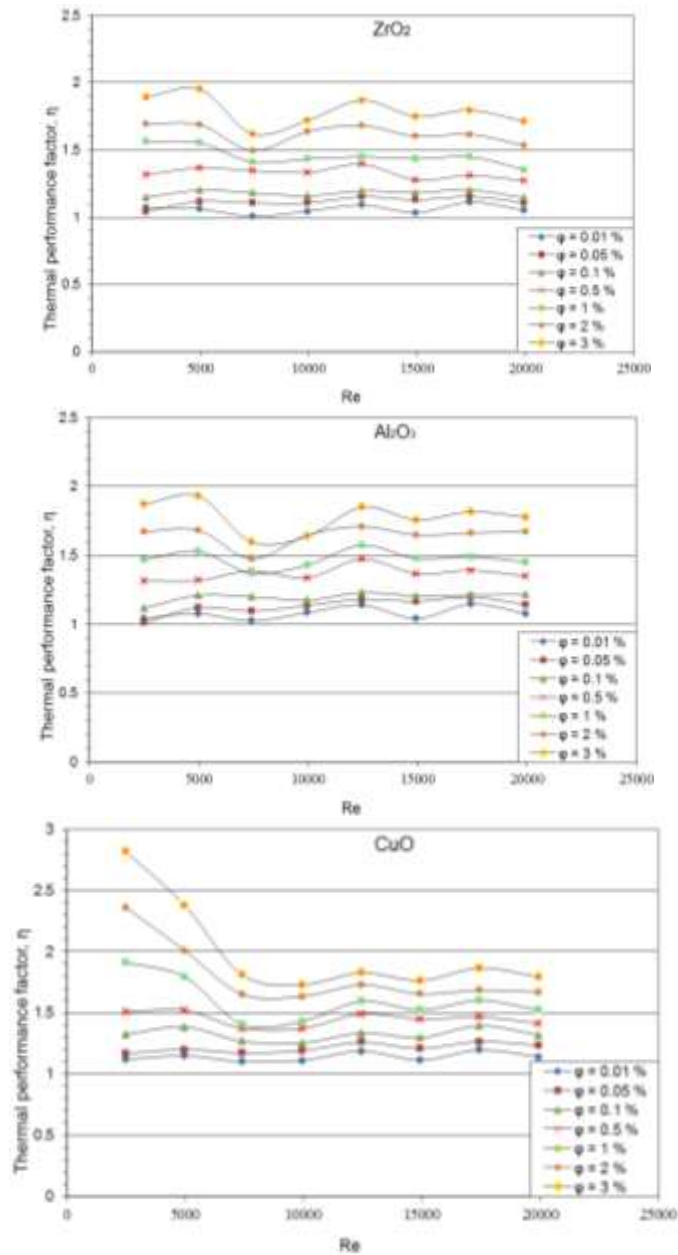


Figure (13) The effect of Reynolds number and twist tape type on thermal performance factor ( $\eta$ ) for ZrO<sub>2</sub>, CuO, Al<sub>2</sub>O<sub>3</sub> nanofluid and for different concentrations in a plain tube

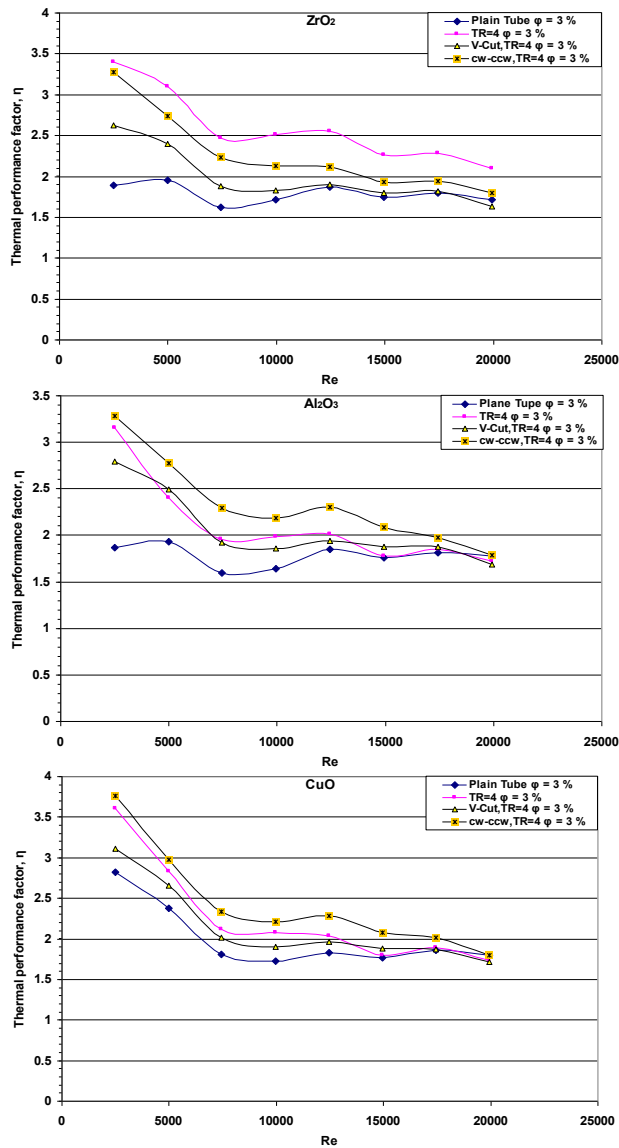


Figure.(14) The effect of Reynolds number and twist tape type on thermal performance factor ( $\eta$ ) for ZrO<sub>2</sub>, CuO, Al<sub>2</sub>O<sub>3</sub> nanofluid and concentrations ( $\phi = 3\%$ )

**CONCLUSIONS**

The twist ratio (TR=4) gives higher Nusselt number compared to (TR=6, 8), and the clockwise-counterclockwise type yields higher Nusselt number compared to the other types. The nanofluid enhances the heat transfer compared with the base fluid (distilled water) under the same Reynolds number, with little increase of pressure drop. The heat transfer enhanced with increasing nanoparticles concentration, and ( $\phi=3\%$ ) gives higher heat transfer enhancement among the studied concentration.

The nanofluid (CuO– distilled water) shows more heat transfer enhancement compared with  $\gamma\text{Al}_2\text{O}_3$  –distilled water and  $\text{ZrO}_2$  – distilled water.

The maximum enhancement in the heat transfer (the Nusselt number ratio) was (3.7) for CuO at Reynolds number (2490) and concentration ( $\phi=3\%$ ).

- The maximum thermal performance factor was for CuO (2.7) at Reynolds number (2490) and concentration ( $\phi=3\%$ ).

The combined use of the nanofluid and twisted tape gives higher heat transfer enhancement compared to the individual use of each one and shows that the maximum enhancement in the heat transfer (7.5 times Nusselt number of the distilled water) and thermal performance factor was (3.9) for CuO with clockwise-counter clockwise twisted tape and twist ratio (TR= 4) at Reynolds number (2490) and concentration ( $\phi=3\%$ ).

**NOMENCLATURE**

SYMBOL	DESCRIPTION	UNITS
A	Surface area of the tube	$\text{m}^2$
C	Specific heat	$\text{kJ/kg.K}$
D	Diameter	m
DR	Depth ratio	-
$d_p$	Particle diameter	nm
$e_d$	V-cut Depth	m
$e_w$	V-cut width	m
h	Heat transfer coefficient	$\text{W/m}^2.\text{K}$
k	Thermal conductivity	$\text{W/m.K}$
K	Boltzmann's constant ( $1.38054 \times 10^{-23}$ )	J/K
$\dot{m}$	Mass flow rate	kg/s
m	Mass	kg
Nu	Nusselt number	-
p	Pressure	$\text{N/m}^2$
P	pitch distance	m
Pr	Prandtl number	-
Q	Volume flow rate	$\text{m}^3/\text{s}$
$\dot{Q}$	Total heat power	W
$\dot{q}$	Heat flux	$\text{W/m}^2$
Re	Reynolds number	-
r	Tube radius	m
T	Temperature	$^\circ\text{C}$
TR	Twist ratio	-
W	Tape width	m
WR	Depth ratio	-
Z	Test section length	m

**Greek Symbols**

SYMBOL	DESCRIPTION	UNITS
$\beta$	Thermal expansion coefficient	1/K
$\gamma$	Crystalline phase	-
$\mu$	Dynamic viscosity	kg/m.s
$\eta$	Thermal performance factor	-
$\rho$	Density	kg/m <sup>3</sup>
$\phi$	Volume fraction	-
f	Friction factor	-

**Subscripts**

SYMBOL	DESCRIPTION
bf	Base fluid
e	Entrance
f	Fluid
in	Inlet
nf	Nanofluid
o	Outer
s	Surface
si	Inner surface
so	Outer surface

**REFERENCES**

- [1] Sarit K., Stephen U. S. Choi, Wenhua Y. and Pradeep T., "NANOFLUIDS :Science and Technology ", 2008 by John Wiley & Sons, Inc.
- [2] Stephen U. S. Choi, "Enhancing Thermal Conductivity of Fluids with nanoparticles", Developments and Applications of Non – Newtonian Flows", American Society of Mechanical Engineers (ASME) 66 (1995), pp. 99.
- [3] Stephen U. S. Choi," Nanofluid technology, current status and future research ", Energy Technology division Reports, Argonne National Laboratory, Argonne,IL.,(1999).
- [4] Lee S, Stephen U. S. Choi, Li S, Eastman JA., "Measuring thermal conductivity of fluids containing oxide nanoparticles", J. of Heat Transfer 1999;121:280–9.
- [5] Wang X, Xu X, Stephen U. S. Choi, "Thermal conductivity of nanoparticle-fluid mixture", J. of Thermophysics and Heat Transfer, 1999,13,474–80.
- [6] Sharma K., Syam Sundar L., Sarma P., "Estimation of heat transfer coefficient and friction factor in the transition flow with low volume concentration of Al<sub>2</sub>O<sub>3</sub> nanofluid flowing in a circular tube and with twisted tape insert". International Communications in Heat and Mass Transfer 2009;36:503–7.
- [7] Sundar L., Sharma K., "Turbulent heat transfer and friction factor of Al<sub>2</sub>O<sub>3</sub> nanofluid in circular tube with twisted tape inserts". International Journal of Heat and Mass Transfer 2010;53:1409–16.

- [8] Sajadi A.R., Kazemi M.H., "Investigation of turbulent convective heat transfer and pressure drop of TiO<sub>2</sub>/water nanofluid in circular tube", *International Communications in Heat and Mass Transfer*, 38, (2011), 1474–1478.
- [9] Khalid F. Sultan, " An Investigation In To Heat Transfer And Flow Of Nanofluids In Circular Tube ", Ph.D thesis, University Of Technology, Mechanical Engineering Department, 2012.
- [10] Syam Sundar L., Naik M.T., Sharma K.V., Singh M.K., Siva Reddy T.Ch., "Experimental investigation of forced convection heat transfer and friction factor in a tube with Fe<sub>3</sub>O<sub>4</sub> magnetic nanofluid", *Experimental Thermal and Fluid Science*, 37, (2012), 65–71.
- [11] Heyhat M.M., Kowsary F., Rashidi A.M., Momenpour M.H., Amrollahi A., "Experimental investigation of laminar convective heat transfer and pressure drop of water-based Al<sub>2</sub>O<sub>3</sub> nanofluids in fully developed flow regime", *Experimental Thermal and Fluid Science*, 44, (2013), 483–489.
- [12] Jianli Wanga, Jianjun Zhu, Xing Zhang, Yunfei Chen , "Heat transfer and pressure drop of nanofluids containing carbon nanotubes in laminar flows", *Experimental Thermal and Fluid Science*, 44, (2013), 716–721.
- [13] Naik M.T., Ranga Janardana G., Syam Sundar L., "Experimental investigation of heat transfer and friction factor with water–propylene glycol based CuO nanofluid in a tube with twisted tape inserts", *International Communications in Heat and Mass Transfer*, 46, (2013), 13–21.
- [14] Murugesan P., Mayilsamy K., Suresh S. and Srinivasan P.S., " Heat transfer and pressure drop characteristics in a circular tube fitted with and without V-cut twisted tape insert ", *International Communications in Heat and Mass Transfer*, 38, (2011), 329–334.
- [15] Raghu Gowda, Hongwei Sun, Pengtao Wang, Majid Charmchi, Fan Gao, Zhiyong Gu, and Bridgette Budhlall, "Effects of Particle Surface Charge, Species, Concentration, and Dispersion Method on the thermal Conductivity of Nanofluids", *Hindawi Publishing Corporation, Advances in Mechanical Engineering*, Volume 2010.
- [16] Molisunora, Nilebovka, OVmelezhyk et al., "Stability of the aqueous Suspensions of nanotubes in the presence Of nonionic Surfactant" [*J.J. Colloid interface sci.*, (2006), 299:740 – 746.
- [17] Xfli, Dszhu, XJ Wang, "Evaluation on dispersion behavior of the aqueous copper nanosuspensions" [*J. J. Colloid interface sci.*, (2007), 310(2); 456 – 463.
- [18] Ravikanth S. Vajjha, Debendra K. Das, "Experimental determination of thermal conductivity of three nanofluids and development of new correlations", *International Journal of Heat and Mass Transfer* 52 (2009) 4675–4682
- [19] Holman J. P., "Heat Transfer", Tenth Edition, 2010 by the McGraw-Hill Companies, Inc.
- [20] Frank M. White, "Fluid Mechanics", Fourth edition, MacGraw-Hill books, 2001.
- [21] Eiamsa-ard S., Wongcharee K., Eiamsa-ard P., and Thianpong C., "Heat transfer enhancement in a tube using delta-winglet twisted tape inserts", *Applied Thermal Engineering*, 30, (2010), 310–318.
- [22] Eiamsa-ard S., Thianpong C., Eiamsa-ard P., "Turbulent heat transfer enhancement by counter/co-swirling flow in a tube fitted with twin twisted tapes", *Experimental Thermal and Fluid Science*, 34, (2010), 53–62.